# A Phenanthrene Condensed Thiadiazoloquinoxaline Donor-Acceptor Polymer for Phototransistor Applications

| | |
|---|---|
| Journal: | *Chemistry of Materials* |
| Manuscript ID: | cm-2015-00341c.R1 |
| Manuscript Type: | Article |
| Date Submitted by the Author: | 05-Mar-2015 |
| Complete List of Authors: | Li, Mengmeng; Max Planck Institute for Polymer Reaserch,<br>An, Cunbin; Max Planck Institute for Polymer Reaserch,<br>Marszalek, Tomasz; Max Planck Institute for Polymer Research,<br>Guo, Xin; Max Planck Institute for Polymer Research,<br>Long, Yun-Ze; Qingdao University, College of Physics<br>Yin, Hong-Xing; Qingdao University, College of Physics Science<br>Gu, Changzhi; Institute of Physics, Chinese Academy of Sciences, Beijing National Laboratory for Condensed Matter Physics<br>Baumgarten, Martin; Max Planck Institute, Polymer research<br>Pisula, Wojciech; Max Planck Institute for Polymer Research,<br>Müllen, Klaus; Max-Planck-Institute for Polymer Research, |
| | |

# A Phenanthrene Condensed Thiadiazoloquinoxaline Donor-Acceptor Polymer for Phototransistor Applications

Mengmeng Li,[†,‡] Cunbin An,[†,‡] Tomasz Marszalek,[‡] Xin Guo,[‡] Yun-Ze Long,[§] Hongxing Yin,[¶] Changzhi Gu,[¶] Martin Baumgarten,[*,‡] Wojciech Pisula,[*,‡] *and* Klaus Müllen[*,‡]

[‡]Max Planck Institute for Polymer Research, Ackermannweg 10, 55128 Mainz, Germany

[§]College of Physics, and State Key Laboratory Cultivation Base of New Fiber Materials & Modern Textile, Qingdao University, 266071 Qingdao, China

[¶]Institute of Physics, Chinese Academy of Sciences, 100190 Beijing, China

Supporting Information

**ABSTRACT:** A novel donor-acceptor polymer, **PPhTQ**, is synthesized by condensing a phenanthrene unit onto a thiadiazoloquinoxaline moiety. This polymer shows a broad absorption band from visible to near infrared and a very low optical bandgap of 0. 80 eV. A well-balanced ambipolar field-effect behavior is observed for **PPhTQ**, with mobilities of 0.09 $cm^2 V^{-1} s^{-1}$ for holes and 0.06 $cm^2 V^{-1} s^{-1}$ for electrons. A two-dimensional charge carrier transport in the film is determined by low-temperature resistance measurements, and an ordered face-on organization is found by grazing incidence wide-angle X-ray scattering. More importantly, a **PPhTQ** thin film phototransistor exhibits an excellent device performance with a maximum photoresponsivity of 400 A/W.

## 1. INTRODUCTION

As key elements for future organic electronics, polymeric field-effect transistors (FETs) are attracting attention due to their advantages such as low cost, light weight, mechanical flexibility and solution processibility. Rational tailoring of the donor (D) and acceptor (A) units is an efficient strategy to manipulate the optoelectronic properties of D-A conjugated polymers. To date, a variety of acceptors with high electron affinity have been designed to construct D-A ambipolar polymer semiconductors, including benzobisthiadiazole (BBT),[1] diketopyrrolopyrrole (DPP),[2] isoindigo (IID),[3] and thiadiazoloquinoxaline (TQ).[4] While few D-A conjugated polymers exhibit high charge carrier mobilities with well-balanced ambipolar transport,[5-7] they are barely used as the active layer of phototransistors.

Phototransistors are a type of photosensitive transistors in which light detection and signal amplification are combined in a single device,[8-10] which have recently seen a significant progress. The photoresponsivity ($P_R$) of organic phototransistors (OPTs) could be improved up to $10^3$ A/W,[11-12] one order of magnitude higher than that of their single-crystal silicon counterpart (~300 A/W).[13] In particular, the $P_R$ value of single-crystal OPTs is as high as $10^4$ A/W.[14-16] In spite of these remarkable achievements, it must be noted that most OPT studies focused on small molecules, while only few reports utilized conjugated polymer as the active layer for OPTs. For traditional polymeric thin film OPTs, the highest $P_R$ value is only 100-250 A/W,[17,18] although higher records were found.[19]

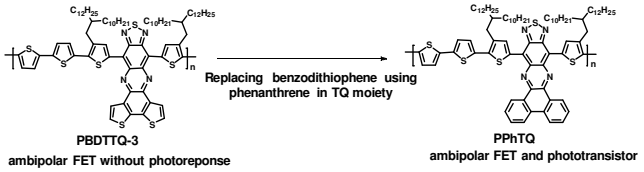


**Figure 1.** Multifunctional TQ-containing polymer.

To realize high-performance phototransistors, three critical processes are required: light-induced generation, transport and collection of charge carriers. Unfortunately, most conjugated polymers have narrow absorption bands and low mobilities, which both lead to low performance of their phototransistors.[10] In contrast, D-A conjugated polymers can harvest more incident photons for efficient generation of charge carriers because of their low bandgap.[20] Herein, we present a newly designed phenanthrene condensed thiadiazoloquinoxaline D-A polymer, **PPhTQ**, which shows a low optical bandgap of 0.80 eV. Furthermore, a well-balanced ambipolar charge carrier transport is observed, with mobilities of 0.09 $cm^2 V^{-1} s^{-1}$ for holes and 0.06 $cm^2 V^{-1} s^{-1}$ for electrons. In comparison to

other high-mobility ambipolar polymers such as DPP polymers[7], this transistor performance is not superior; more importantly, however, **PPhTQ** is found to act as an effective active layer for OPT devices. The maximum $P_R$ value of 400 A/W is higher than that of single-crystal silicon and thus among the best performing polymeric thin film phototransistors.

## 2. EXPERIMENTAL SECTION

*General method:* $^1$H NMR and $^{13}$C NMR spectra were recorded in deuterated solvents on a Bruker DPX 250. High Resolution Mass Spectra (HRMS) were performed by the Microanalytical Laboratory of Johannes Gutenberg-University, Mainz. Elemental analysis was carried out using a Foss Heraeus Vario EL in the Institute of Organic Chemistry at the Johannes Gutenberg-University, Mainz. UV–Vis-NIR absorption spectra were measured on a Perkin-Elmer Lambda 9 spectrophotometer at room temperature. Thermogravimetry analysis (TGA) was carried out on a Mettler 500 Thermogravimetry Analyzer. Cyclic Volatammetry (CV) was measured on a computer-controlled GSTAT12 in a three-electrode cell in anhydrous solvents solution of n-$Bu_4NPF_6$ (0.1 M) with a scan rate of 50 mV/s at room temperature under argon (dichloromethane for **PhTQ** and acetonitrile for **PPhTQ**). A Pt wire, a silver wire, and a glassy carbon electrode were used as the counter electrode, the reference electrode, and the working electrode, respectively. For **PhTQ**, the measurement was carried out using a 0.1 mol/L dichloromethane solution of n-Bu4NPF6 as electrolyte, while **PhTQ** was dissolved with a concentration of $10^{-3}$ mol/L. The electron affinity (EA) was estimated from the onset of the first reduction peak, while the potentials were determined using ferrocene (Fc) as standard by the empirical formula EA = - ($E_{Red}^{onset}$-$E_{Fc/Fc+}^{1/2}$+4.8) eV wherein $E_{Fc/Fc+}^{1/2}$ = 0.63 eV (measured from our setup). The molecular weight was determined by PSS-WinGPC (PSS) (pump: alliance GPC 2000) GPC equipped with an UV or RI detector running in THF at 30 °C using a PLgel MIXED-B column (particle size: 10 mm, dimension: 0.8×30 cm) calibrated against polystyrene standards. Density functional theory (DFT) calculations were performed by the Gaussian 03[21] program with the B3LYP hybrid functional and basis set 6-31G for the ground state geometry optimization[22,23].

*Substrate modification by SAM:* The heavily doped silicon wafers with a 300-nm-thick thermal oxide layer on top were used as substrates, which were cleaned by 10 min ultrasonication in acetone and subsequent 10 min ultrasonication in isopropanol. After activation by using oxygen plasma, the substrates were functionalized with a self-assembled monolayer of hexamethyldisilazane (HMDS, Alfa) from the vapor phase using a vapor prime system at 140 $^oC$ for 6 h.

*Characterization*: A Digital Instruments Nanoscope IIIa Atomic Force Microscopy (AFM) in tapping mode was utilized to record the morphology of drop-cast films. The temperature dependence of the resistance of the thin film was measured by PPMS (Physical Property Measurement System, Quantum Design). GIWAXS experiments were performed by means of a solid anode X-ray tube (Siemens Kristalloflex X-ray source, copper anode X-ray tube operated at 35kV and 40mA). Osmic confocal MaxFlux optics, X-ray beam with pinhole collimation and a MAR345 image plate detector. The beam size was 0.5 × 0.5 mm and samples were irradiated just below the critical angle for total reflection with respect to the incoming X-ray beam (~ 0.18°). The samples were prepared as thin film following the same procedure as it was used for FETs.

*Device Fabrication and Measurements:* Bottom-gate bottom-contact architecture was utilized for FET devices. The source and drain electrodes with 60 nm in thickness were deposited by Au evaporation. Before the measurement, annealing at 180 $^oC$ was carried out to remove residual solvent. A Keithley 4200-SCS was used for all electrical measurements in a glovebox under nitrogen atmosphere. The white light of a Nikon microscope (SMZ1000, ~15 mW/cm$^2$) was directly used for irradiation.

*Synthetic details*: All chemicals and reagents were used as received from commercial sources without further purification unless stated otherwise. Compounds 4,7-bis(4-(2-decyltetradecyl)thiophen-2-yl)-5,6-dinitrobenzo[c][1,2,5]thiadiazole (**1**) and 5,5'-bis(trimethylstannyl)-2,2'-bithiophene (**4**) were prepared according to our previous procedures.[25]

**10,14-Bis(4-(2-decyltetradecyl)thiophen-2-yl)dibenzo[a,c][1,2,5]thiadiazolo[3,4-i]phenazine (PhTQ):** Compound **1** (0.5 g, 0.47 mmol) and fine iron powder (311 mg, 5.55 mmol) in acetic acid (15 mL) were stirred for 5 h at 75 °C under argon. Then the reaction mixture was cooled to room temperature, and poured into 50 mL of water. 5% NaOH aqueous solution was carefully added until pH value reaches 7. The mixture was extracted with diethyl ether for 3 times. The combined organic layers were washed with brine, dried with $MgSO_4$ and the solvent was removed under reduced pressure to give the corresponding diamine **2** as deep dark oil. This crude product was directly added into an acetic acid (15 mL) solution of phenanthrene-9,10-dione (97.8 mg, 0.47 mmol). The mixture was heated to 80 °C overnight under argon. After cooling to room temperature, the mixture was poured into 100 mL 5% aqueous NaOH and extracted with dichloromethane. The combined organic phases were dried with $MgSO_4$ and filtered. The filtrate was concentrated and purified by column chromatography eluting with hexane dichloromethane (3:1) to give 0.32 g (green solid, two steps 58%) of **PhTQ**. $^1$H NMR (250 MHz, $CD_2Cl_2$, ppm) δ 9.30 (dd, *J*= 2.5 Hz, *J* = 7.5 Hz, 2H), 8.78 (s, 2H), 8.38 (dd, *J* = 2.5 Hz, *J* = 7.5 Hz, 2H), 7.74-7.61 (m, 4H), 7.27 (d, *J* = 2.5 Hz, 2H), 2.70 (d, *J* = 7.50 Hz, 4H), 1.80 (br, 2H), 1.40-1.22 (br, 80H), 0.87-0.82 (m, 12H). $^{13}$C NMR (62.5 MHz, $CD_2Cl_2$, ppm) δ 151.58,

**Scheme 1.** Synthetic route for **PPhTQ**.[a]

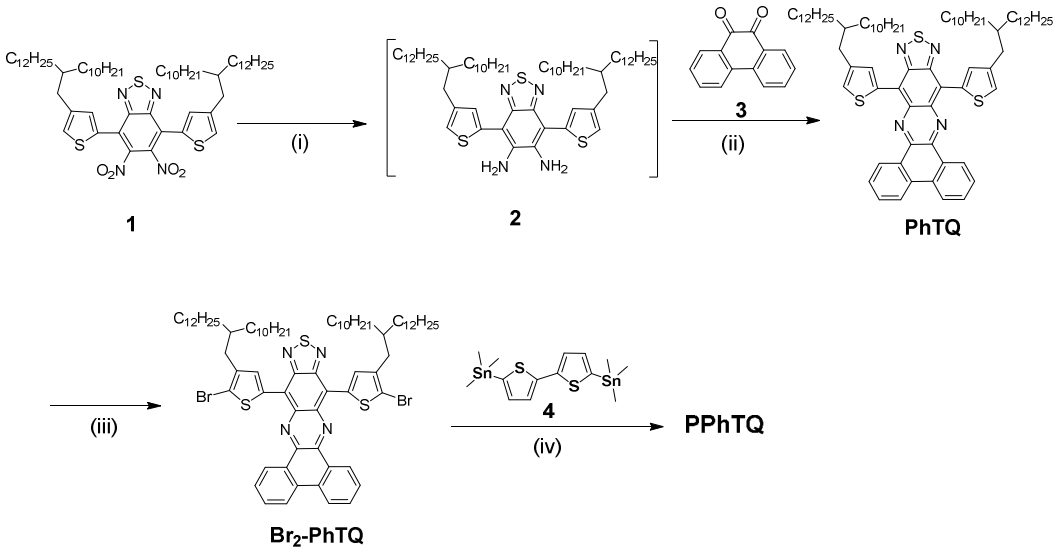


[a]Reagents and conditions: (i) Fe, $CH_3COOH$; (ii) $CH_3COOH$, phenanthrene-9,10-dione, 58% (two steps); (iii) NBS, THF, 87%; (iv) Chlorobenzene, $Pd_2(dba)_3$, tri(o-tolyl)phosphine, 50 %.

143.65, 141.82, 136.07, 135.88, 135.85, 133.17, 131.33, 130.61, 129.15, 128.49, 127.95, 123.20, 121.06, 39.49, 35.26, 32.34, 30.59, 30.21, 30.19, 30.16, 30.14, 30.12, 30.08, 29.81, 29.78, 27.12, 23.10, 14.29. HRMS (ESI+): m/z calc. 1175.7971 found 1175.7993.

**10,14-Bis(5-bromo-4-(2-decyltetradecyl)thiophen-2-yl)dibenzo[a,c][1,2,5]thiadiazolo[3,4-i]phenazine ($Br_2$-PhTQ)**: **PhTQ** (284 mg, 0.24 mmol) was dissolved in 15 mL THF at room temperature. NBS (94 mg, 0.53 mmol) was carefully added into the solution in small batches in the dark. After stirring for 5 h, the solvent was removed under reduced pressure. The residue was then purified by column chromatography with eluent dichloromethane/hexane (1:3) to give **$Br_2$-PhTQ** as a green solid (280 mg, 87%). $^1$H NMR (250 MHz, $CD_2Cl_2$, ppm) δ 8.48 (d, *J* = 7.5 Hz, 2H), 8.34 (s, 2H), 7.84 (d, *J* = 10.0 Hz, 2H), 7.30 (t, *J* = 7.5 Hz, 2H), 7.12 (t, *J* = 7.5 Hz, 2H), 2.36 (d, *J* = 7.0 Hz, 4H), 1.71 (m, 2H), 1.36-1.24 (br, 80H), 0.87 (t, *J* = 7.50 Hz, 12H). $^{13}$C NMR (62.5 MHz, $CD_2Cl_2$, ppm) δ 150.38, 142.95, 140.40, 135.20, 135.01, 134.75, 132.46, 130.85, 129.51, 128.92, 127.81, 122.46, 119.22, 118.74, 38.95, 34.16, 33.76, 32.41, 32.38, 30.72, 30.32, 30.29, 30.25, 30.22, 30.20, 30.15, 29.88, 29.84, 27.02, 23.15, 23.13, 14.35. HRMS (ESI+): m/z calc. 1331.6181, found 1331.6171.

**PPhTQ**: **$Br_2$-PhTQ** (0.1 mmol), compound **4** (0.1 mmol), and chlorobenzene (8 mL) were placed in a 50 mL Schlenk tube. The mixture was purged with argon for 5 min, and then 5.5 mg of tris(dibenzylideneacetone)dipalladium(0) ($Pd_2(dba)_3$) and 7.3 mg of tri(*o*-tolyl)phosphine (P(*o*-tolyl)3) were added. Then the mixture was heated to 110 °C under argon for 3 days. The polymer was end-capped with tributylphenylstannane and bromobenzene in sequence. After cooling to room temperature, the reaction mixture was poured into methanol. The polymer was filtered and subjected to Soxhlet extraction with methanol, acetone, hexane, dichloromethane and chloroform. 30 mL of sodium diethyldithiocarbamate aqueous solution (1 g/100 ml) was added into the chloroform fraction to remove residual palladium catalyst. The mixture was heated to 60 °C with vigorous stirring for 2 h. The mixture was separated and the organic phase was washed with water for 3 times. The chloroform solution was concentrated and precipitated in methanol. The target polymer was collected by filtration and dried in vacuum to afford a black solid 61 mg (50%). Molecular weight by GPC: $M_n$ = 37.2K (g/mol), $Đ$ = 1.88. Anal. Calcd for $C_{84}H_{112}N_4S_5$: C, 75.42; H, 8.44; N, 4.19; S, 11.95. Found: C, 75.08; H, 9.41; N, 3.91; S, 11.56.

## 3. RESULTS AND DISCUSSION

**PPhTQ** is designed according to our previous work.[25] We developed a new acceptor unit, benzodithiophene-thiadiazoloquinoxaline (**BDTTQ**), and used it to construct an ambipolar polymer, **PBDTTQ-3** (Figure 1).[25] To enhance the practical applications of such polymers in organic electronics, a photosensitizer group, phenanthrene,[26,27] is attached onto the TQ moiety to replace the benzodithiophene group in **PBDTTQ-3**. The synthesis of **PPhTQ** is shown in Scheme 1. The compound **1** is converted to the corresponding diamine **2**, which is not purified and directly condensed with phenanthrene-9,10-dione to give monomer **PhTQ**. Afterwards, the dibromination is carried out to obtain **$Br_2$-PhTQ**. Finally, **PPhTQ** is prepared via Stille coupling between **$Br_2$-PhTQ** and distannylbithiophene **4**. The detailed synthesis is depicted in the experimental section. **PPhTQ** shows a good solubility in common solvents such as chloroform, tetrahydrofuran (THF) and toluene. An average molecular weight ($M_n$) of 37.2 kg/mol and a polydispersity index ($Đ$) of 1.88 are determined by GPC using polystyrene as standard and THF as eluent at 30 °C, as shown in Table S1. It is worth noting that this is a **PhTQ** containing polymer with the highest molecular weight achieved so far.[28] Additionally, this polymer

exhibits an excellent thermal stability with only 5% weight loss at 402 °C (Figure S1).

UV-Vis-NIR absorption spectra of **PPhTQ** are measured in dilute toluene solution as well as thin film, and are shown in Figure 2a. A maximum absorption peak at 1143 nm in solution is obviously corresponding to a significant blue-shift of 127 nm as compared to **PBDTTQ-3**.[25] The **PPhTQ** thin film on a glass slide drop-cast from toluene solution displays slightly broadened bands compared to the solution. This broadening indicates aggregation in solid state. The optical bandgap of 0.80 eV is estimated from the absorption onset of the solid film.

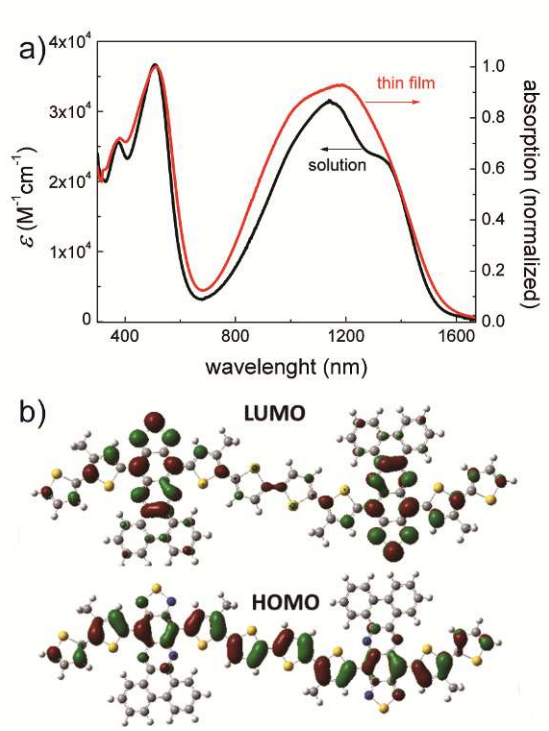


**Figure 2.** a) UV-Vis-NIR absorption spectra of **PPhTQ** in toluene solution and in film, b) LUMO and HOMO diagrams of methyl substituted dimer of the **PPhTQ** repeat unit calculated by DFT (B3LYP, 6-31G*).

The ionization potential (IP) and electron affinity (EA) of **PPhTQ** are calculated from onsets of first oxidation and reduction peaks in the cyclic voltammetry (CV) plots, with values of -5.08 and -4.01 eV (Figure S2). Meanwhile, the electron-withdrawing ability of **PhTQ** is also estimated from CV with the EA value of -3.84 eV (Figure S3). This value is higher than that of **BDTTQ-3** (-3.92 eV) (chemical structure in Figure S4), implying a slightly weaker electron affinity than **BDTTQ-3**.[25] On the other hand, density functional theory (DFT) calculations are also carried out to describe the electron density distribution along the **PPhTQ** backbone, as shown in Figure 2b. The electron density distributions of the LUMO and HOMO levels of dimer of **PPhTQ** repeat units are similar to **PBDTTQ-3**. These results imply a potential for ambipolarity of **PPhTQ**. In comparison with the optical bandgap, the electrochemical bandgap increases by 0.27 eV, which might result from the exciton bonding energy of the conjugated polymer.[24]

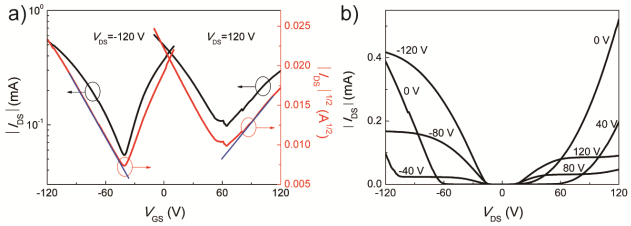


**Figure 3.** Typical a) transfer and b) output curves in the saturation regime of **PPhTQ** transistors drop-cast from 10 mg/mL chloroform solution on HMDS-modified substrate. Blue lines in a) indicate fits used to extract the mobility values. (see supporting information)

To evaluate the charge carrier transport of **PPhTQ**, thin-film transistors are fabricated with bottom-gate bottom-contact (BGBC) configurations. Heavily doped silicon covered by 300-nm-thick thermally grown oxide dielectric acts as gate electrode and hexamethyldisilazane (HMDS) is employed to functionalize the dielectric surface in order to minimize interfacial trapping sites. Source and drain electrodes are fabricated by Au evaporation. **PPhTQ** thin films with the thickness of 1-5 μm are deposited by drop-casting from 10 mg/mL chloroform solution. Figure 3 presents the transfer and output characteristics in the saturation regime. More importantly, a well-balanced ambipolar charge carrier transport is evident from the transfer curve in both p- and n-type operation modes for negative and positive gate voltages. In the negative drain mode for a source-drain voltage ($V_{DS}$) of -120 V, the crossover point is located at around $V_{GS}$ = -40 V indicating a change from electron- to hole-dominated current (Figure 3a). Below this $V_{GS}$ the transistor exhibits a hole transport in the accumulation mode. In the positive regime at $V_{DS}$ = 120 V the electrons dominate the device operation from approximately $V_{GS}$ = 60 V, which is slightly improved in comparison to **PBDTTQ-3** (70 V).[25] This relatively high turn-on voltage may result from the immobile Si–O$^-$ ions at the semiconductor/dielectric interface caused by electrochemically trapping the injected electrons.[29] Although the charge trapping can be alleviated by HMDS, it cannot be completely eliminated. It has been proven that this negative effect influences only the threshold voltage, but not the mobility.[30] A stronger hysteresis for electron transport is observed indicating a higher density of trapping sites for electrons (Figure S5).[31] On the other hand, at low $V_{DS}$ the output plots exhibit a large $I_{DS}$ offset which is defined as the drain current at different $V_{GS}$ and $V_{DS}$= 0 V, resulting from the gate-induced leakage current (Figures 3b and S6).[32] The saturation field-effect mobilities of **PPhTQ** reach values of 0.09 cm$^2$ V$^{-1}$ s$^{-1}$ for holes and 0.04 cm$^2$ V$^{-1}$ s$^{-1}$ for electrons, which are among the best transistor performances for TQ-containing polymers.[25] In addition, the electron transport is slightly enhanced reaching a saturation mobility of 0.06 cm$^2$ V$^{-1}$ s$^{-1}$ when chlorobenzene is used as solvent. The on/off ratio of the devices is as low as 10-10$^2$, which could be ascribed to the adventitious doping due to the high IP value of this polymer.[33] The mobilities in the linear regime are also investigated with slightly lower

values of 0.07 $cm^2 V^{-1} s^{-1}$ for holes and 0.04 $cm^2 V^{-1} s^{-1}$ for electrons (Figure S7).

The charge carrier transport in a **PPhTQ** thin film is also investigated by a low-temperature resistance measurement. The electric field is only applied between source and drain electrodes, and two different bias voltages (1 and 20 V) are employed. The temperature dependence of the film resistance is shown in Figure 4. The resistance follows the exponential temperature dependence of variable range hopping (VRH).[34] In this model, the conductance of carriers is controlled by the electrons between local states nearby the Fermi level: $R(T)=R_o \cdot \exp(T_o/T)^m$, where $R$ is the resistance; the exponent m=1/2, 1/3, and 1/4 represent one-dimensional (1D), two-dimensional (2D), and three-dimensional (3D) hopping, respectively; $T_o$ is the Mott characteristic temperature, and can be obtained from the $\ln R(T) \sim T^{-1/m}$ plots. It has to be emphasized that this model includes some structural information at the molecular level without taking the mesoscale microstructure into account.[35] The $R(T)$ data of the **PPhTQ** film at both bias voltages are well fitted by the 2D-VRH model: $R(T)=R_o \cdot \exp(T_o/T)^{1/3}$. In other words, the charge carrier transport in the **PPhTQ** film occurs in two dimensions. The Mott characteristic temperature $T_o$ obtained from Figure 4 is about $7.87 \times 10^6$ K, which is much larger than those of conducting polymers (usually less than $10^5$ K), indicating a higher conduction barrier in the **PPhTQ** films.

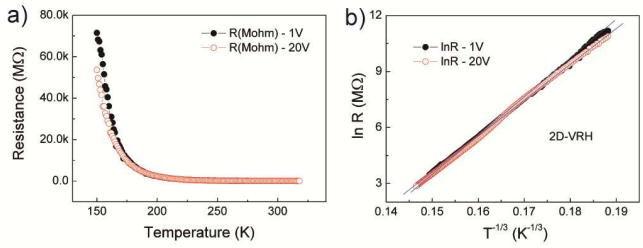


**Figure 4.** a) Temperature dependence of the film resistance (film spin-coated from chlorobenzene) with the bias of 1 and 20 V, b) curves of a) are plotted as $\ln R(T) \propto T^{-1/3}$.

The morphology of the drop-cast **PPhTQ** film is determined by atom force microscopy (AFM) in tapping-mode, as presented in Figure 5a. **PPhTQ** film displays aggregated granular topography which is similar with other reported TQ polymers.[25] The domain size is ranging from 50 to 100 nm with the surface root-mean-square roughness of 3.05 nm. These large domains create sufficient pathways for charge carrier transport resulting in relatively high OFET performance. To elucidate the molecular organization in **PPhTQ** thin films, grazing-incidence wide-angle X-ray scattering (GIWAXS) is performed, as shown in Figure 5b. The GIWAXS pattern exhibits a pronounced order which is evident from reflections up to second order appearing in the out-of-plane pattern. From the first order peak at $q_z$ = 0.25 $Å^{-1}$ and $q_{xy}$= 0 $Å^{-1}$ an interlayer distance of 2.51 nm is determined (reflection R1 in Figure S8). Additional reflections at $q_z$=0 $Å^{-1}$ and $q_{xy}$=0.32 $Å^{-1}$ corresponding to a d-spacing of 1.96 nm and located on the equatorial plane are assigned to the length of the repeating unit along the backbone (reflection R5 in Figure S8). The reflection at the wide-angle out-of-plane is related to the π-stacking distance of 0.375 nm (reflection R4 in Figure S8). The appearance of the interlayer and π-stacking reflection on the same plane indicates the coexistence of the face- and edge-on organization, whereby the first type of arrangement reveals a π-stacking peak in the GIWAXS pattern. In contrast, as previously reported, **PBDTTQ-3** possesses only poor order in spite of its similar chemical structure and FET performance to **PPhTQ**. Since the **PPhTQ** polymer leads to a pronounced ambipolar behavior despite its face-on arrangement, it can be assumed that the charge transport also takes place along polymer conjugated backbone.[36,37]

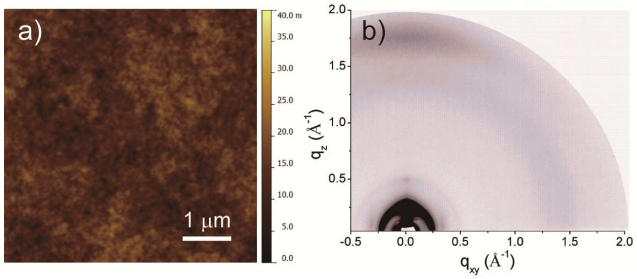


**Figure 5.** a) AFM image and b) GIWAXS pattern for **PPhTQ** thin films on a HMDS-modified substrate.

In comparison to the recently reported TQ-containing polymers such as **PBDTTQ-3**,[25] **PPhTQ** exhibits an identical ambipolar transistor performance. However, the introduction of the phenanthrene group results in an additional high photoresponsivity opening great potential for OPT applications. Figure 6a exhibits its device performance as a phototransistor. At $V_{GS}=V_{DS}$= -80 V, the absolute value of the drain current is around 200 μA in the dark. When light is switched on, the absorption of the light generates hole-electron pairs. The photogenerated holes can easily move to the drain electrode under the action of the electrical field between source and drain.[38] As reported in the literature, the photogenerated electrons are trapped under the source electrode.[38] Interestingly, the electrons lower the potential barrier between the source and channel and consequently facilitate the injection of excess holes from the source electrode into the organic semiconductor layer.[38] As a result, a photocurrent ($I_{ph}$) of ~100 μA is generated so that $-I_{DS}$ increases to ~300 μA. After switching off the light, the drain current is reduced to the original level. The stability of **PPhTQ** phototransistors is confirmed by 7 on-off cycles (Figure 6a). A single cycle of the photoresponse behavior is presented in Figure S9. Photoresponsivity ($P_R$) and photosensitivity ($P_S$) are key parameters for assessing the performance of phototransistors. The values of $P_R$ and $P_S$ are typically defined as: $P_R = (I_{inc}-I_{dark})/P_{inc} = I_{ph}/P_{inc}$, $P_S = (I_{inc}-I_{dark})/I_{dark} = I_{ph}/I_{dark}$, where $P_{inc}$ is the incident illumination power on the device channel, $I_{inc}$ and $I_{dark}$ are the drain current under the incident illumination and in the dark, respectively. $P_R$ is plotted as a function of the gate voltage ($V_{GS}$) with $V_{DS}$= -80 V in Figure 6b. At $V_{GS}$< 0 V, $P_R$ is only around 0.1 A/W, while this parameter significantly grows to 400 A/W with increasing $V_{GS}$ to -80 V. To the best of our knowledge, this value exceeds that of single-crystal silicon

and is among the highest photoresponsivity for thin film phototransistors based on conjugated polymers.[17] There are three possible reasons for such high OPT performance.[39] Firstly, **PPhTQ** shows a broad absorption band from visible to near infrared. Secondly, the IP energy level (-5.08 eV) of this polymer is close to the work function of Au electrodes (~-5.1 eV). Thirdly, the charge carrier mobility of this polymer is pronounced. The value of $P_S$ is comparably low, with a maximum value of about 0.5 (Figure S10), which is primarily attributed to the high off-current and subsequent low on/off ratio of **PPhTQ**. It is assumed that such photoelectric property of this polymer originates from the new TQ moiety, **PhTQ**.

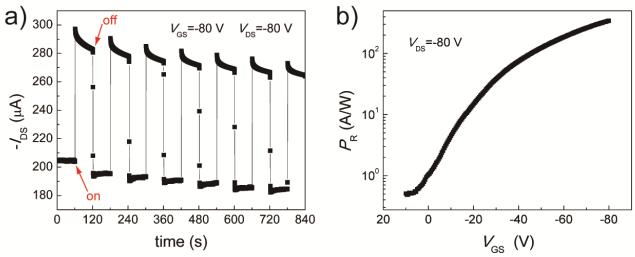


**Figure 6.** a) On-off characteristics of the phototransistor at $V_{GS}$=-80 V and $V_{DS}$=-80 V. "On" and "off" are related to light switching. b) Variation of photoresponsivity $P_R$ with $V_{GS}$ at $V_{DS}$=-80 V.

### 4. CONCLUSION

A new TQ-based conjugated polymer, **PPhTQ**, is synthesized. The introduction of a phenanthrene group into the TQ moiety has only a slight influence on the charge carrier transport in comparison to the other recently reported TQ-based polymers.[25] **PPhTQ** still exhibits a well-balanced ambipolor field-effect behavior with mobilities of 0.09 $cm^2 V^{-1} s^{-1}$ for holes and 0.06 $cm^2 V^{-1} s^{-1}$ for electrons. Interestingly, this structural modification opens up the application of **PPhTQ** as an active layer in OPT devices. The resulting thin film phototransistor shows a maximum photoresponsivity of 400 A/W, which not only exceeds that of single-crystal silicon-based OPTs (~300 A/W), but is also among the best thin-film OPT performances for conjugated polymers. Photodetection with ultra-broadband from the ultraviolet (UV)-visible to the infrared is of vital importance in both industrial and scientific fields, such as spectroscopy, communications, environmental monitoring, remote control, and chemical/biological sensing.[40] It has to be emphasized that a strong and broad absorption in the near-infrared (700-1500 nm, Figure 2a) is also observed for **PPhTQ** besides the visible light, which makes the polymer potentially applicable for the detection of the near infrared. Now we are investigating **PPhTQ** phototransistors within a broad wavelength range from visible to near-infrared, which can reinforce our confidence for the practical applications of organic semiconductors, especially conjugated polymers.

## ASSOCIATED CONTENT

**Supporting Information**.

Detail of materials characterization and the spectra of TGA, cyclic voltammograms and NMR. This material is available free of charge via the Internet at http://pubs.acs.org.

## AUTHOR INFORMATION

### Corresponding Author

*pisula@mpip-mainz.mpg.de (W. P.); baumgarten@mpip-mainz.mpg.de (M. B.); muellen@mpip-mainz.mpg.de (K. M.)

### Author Contributions

M. L. and C. A. designed and carried out the experiments. W. P., M. B. and K. M. supervised this project. T. M. measured GIWAXS. Y. L., H. Y. and C. G. characterized the low-temperature electric properties. All authors have given approval to the final version of the manuscript. †M. L. and C. A. contributed equally.

### Notes

The authors declare no competing financial interests.

## ACKNOWLEDGMENT

M. L. and T. M. acknowledge the financial support from ERC-Adv.-Grant 267160 (NANOGRAPH), and C. A acknowledges the financial support from China Scholarship Council (CSC). M. B. acknowledges the financial support from SFB-TR49. Y. L. acknowledges the support from National Natural Science Foundation of China (51373082) and Taishan Scholars Program of Shandong Province, China (ts20120528).

## REFERENCES

(1) Fan, J.; Yuen, J. D.; Cui, W.; Seifter, J.; Mohebbi, A. R.; Wang, M.; Zhou, H.; Heeger, A.; Wudl, F. *Adv. Mater.* **2012**, *24*, 6164.
(2) Kang, I.; An, T. K.; Hong, J.-a.; Yun, H.-J.; Kim, R.; Chung, D. S.; Park, C. E.; Kim, Y.-H.; Kwon, S.-K. *Adv. Mater.* **2013**, *25*, 524.
(3) Lei, T.; Dou, J.-H.; Pei, J. *Adv. Mater.* **2012**, *24*, 6457.
(4) Dallos, T.; Beckmann, D.; Brunklaus, G.; Baumgarten, M. *J. Am. Chem. Soc.* **2011**, *133*, 13898.
(5) Chen, Z.; Lee, M. J.; Ashraf, R. S.; Gu, Y.; Albert-Seifried, S.; Nielsen, M. M.; Schroeder, B.; Anthopoulos,T. D.; Heeney, M.; McCulloch, I.; Sirringhaus, H. *Adv. Mater.* **2012**, *24*, 647.
(6) Fan, J.; Yuen, J. D.; Wang, M.; Seifter, J.; Seo, J. H.; Mohebbi, A. R.; Zakhidov, D.; Heeger, A.; Wudl, F. *Adv. Mater.* **2012**, *24*, 2186.
(7) Lee, J.; Han, A. R.; Yu, H.; Shin, T. J.; Yang, C.; Oh, J. H. J. *J. Am. Chem. Soc.* **2013**, *135*, 9540.
(8) Mok, S. M.; Yan, F.; Chan, H. L. W. *Appl. Phys. Lett.* **2008**, *93*, 023310.
(9) Baeg, K.-J.; Binda, M.; Natali, D.; Caironi, M.; Noh, Y.-Y. *Adv. Mater.* **2013**, *25*, 4267.
(10) Dong, H.; Zhu, H.; Meng, Q.; Gong, X.; Hu, W. *Chem. Soc. Rev.* **2012**, *41*, 1754.
(11) Cho,M. Y.; Kim, S. J.; Han, Y. D.; Park, D. H.; Kim, K. H.; Choi, D. H. Joo, J. *Adv. Funct. Mater.* **2008**, *18*, 2905.
(12) Guo, Y.; Du, C.; Di, C.-a.; Zheng, J.; Sun, X.; Wen, Y.; Zhang, L.; Wu, W.; Yu, G.; Liu, Y. *Appl. Phys. Lett.* **2009**, *94*, 143303.
(13) Johnson, N. M.; Chiang, A. *Appl. Phys. Lett.* **1984**, *45*, 1102.

(14) Guo, Y.; Du, C.; Yu, G.; Di, C.-a.; Jiang, S.; Xi, H.; Zheng, J.; Yan, S.; Yu, C.; Hu, W.; Liu, Y. *Adv. Funct. Mater.* **2010**, *20*, 1019.
(15) Kim, K. H.; Bae, S. Y.; Kim, Y. S.; Hur, J. A.; Hoang, M. H.; Lee, T. W.; Cho, M. J.; Kim, Y.; Kim, M.; Jin, J.-I.; Kim, S.-J.; Lee, K.; Lee, S. J.; Choi, D. H. *Adv. Mater.* **2011**, *23*, 3095.
(16) Hoang, M. H.; Kim, Y.; Kim, M.; Kim, K. H.; Lee, T. W.; Nguyen, D. N.; Kim, S.-J.; Lee, K.; Lee, S. J.; Choi, D. H. *Adv. Mater.* **2012**, *24*, 5363.
(17) Pal, T.; Arif, M.; Khondaker, S. I. *Nanotechnology* **2010**, *21*, 325201.
(18) Liu, Y.; Shi, Q.; Ma, L.; Dong, H.; Tan, J.; Hu, W.; Zhan, X. *J. Mater. Chem. C.* **2014**, *2*, 9505.
(19) (a) Liu, Y.; Dong, H.; Jiang, S.; Zhao, G.; Shi, Q.; Tan, J.; Jiang, L.; Hu, W.; Zhan, X. *Chem. Mater.* **2013**, *25*, 2649; (b) Li, H.; Wu, Y.; Wang, X.; Kong, Q.; Fu, H. *Chem. Commun.* **2014**, *50*, 11000.
(20) (a) Liu, Y.; Wang, H.; Dong, H.; Tan, J.; Hu, W.; Zhan, X. *Macromolecules* **2012**, *45*, 1296; (b) Gunes, S., Neugebauer, H.; Sariciftci, N. S. *Chem. Rev.* **2007**, *107*, 1324; (c) Beaujuge, P. M.; Pisula, W.; Tsao, H. N.; Ellinger, S.; Müllen, K.; Reynolds, J. R. *J. Am. Chem. Soc.* **2009**, *131*, 7514; (d) Mas-Torrent, M.; Hadley, P.; Crivillers, N.; Veciana, J.; Rovira, C. *ChemPhysChem* **2006**, *7*, 86.
(21) Frisch, M. J. et al, *Gaussian 03, Revision B.04*, Gaussian, Inc., Pittsburgh PA, **2003**.
(22) Becke, A. D. *J. Chem. Phys.* **1993**, *98*, 1372.
(23) Lee, C.; Yang, W.; Parr, R. G. *Phys. Rev. B* **1988**, *37*, 785.
(24) Sariciftci, N. S. *Primary Photoexcitations in Conjugated Polymers: Molecular Excitons vs Semiconductor Band Model*, World Scientific, Singapore, **1997**.
(25) An, C.; Li, M.; Marszalek, T.; Li, D.; Berger, R.; Pisula, W.; Baumgarten, M. *Chem. Mater.* **2014**, *26*, 5923.
(26) Matsui, J.; Mitsuishi, M.; Aoki, A.; Miyashita, T. *Angew. Chem. Int. Edit.* **2003**, *42*, 2272.
(27) (a) Matsui, J.; Mitsuishi, M.; Aoki, A.; Miyashita, T. *J. Am. Chem. Soc.* **2004**, *126*, 3708; (b) Mitsuishi, M.; Matsui, J.; Miyashita, T. *J. Mater. Chem.* **2009**, *19*, 325.
(28) (a) Hai, J.; Yu, W.; Zhu, E.; Bian, L.; Zhang, J.; Tang, W. *Thin Solid Films* **2014**, *562*, 75; (b) Hai, J.; Shi, G.; Yu, J.; Zhu, E.; Bian, L.; Ma, W.; Tang, W. *New J. Chem.* **2014**, *38*, 4816; (c) Qin, C.; Fu, Y.; Chui, C.-H.; Kan, C.-W.; Xie, Z.; Wang, L.; Wong, W.-Y. *Macromol. Rapid Commun.* **2011**, *32*, 1472.
(29) Chua, L.-L.; Zaumseil, J.; Chang, J.-F.; Ou, E. C. W.; Ho, P. K. H.; Sirringhaus, H.; Friend, R. H. *Nature* **2005**, *434*, 194.
(30) Braga, D.; Horowitz, G. *Adv. Mater.* **2009**, *21*, 1473.
(31) Jones, B. A.; Facchetti, A.; Wasielewski M. R.; Marks, T. J. *J. Am. Chem. Soc.* **2007**, *129*, 15259.
(32) Jia, H.; Pant, G. K.; Gross E. K.; Wallace, R. M.; Gnade, B. E. *Org. Electron.* **2006**, *7*, 16.
(33) Zhang, X.; Steckler, T. T.; Dasari, R. R.; Ohira, S.; Potscavage, W. J.; Tiwari, S. P.; Coppee, S.; Ellinger, S.; Barlow, S.; Bredas, J.-L.; Kippelen, B.; Reynolds, J. R.; Marder, S. R. *J. Mater. Chem.* **2010**, *20*, 123.
(34) (a) Long, Y.; Zhang, L.; Chen, Z.; Huang, K.; Yang, Y.; Xiao, H.; Wan, M.; Jin, A.; Gu, C. *Phys. Rev. B* **2005**, *71*, 165412; (b) Long, Y. Z.; Chen, Z. J.; Wang, N. L.; Zhang, Z. M.; Wan, M. X. *Physica B* **2003**, *325*, 208.
(35) (a) Salleo, A. *Materials Today* **2007**, *10*, 38; (b) Vissenberg, M. C. J. M.; Matters, M. *Phys. Rev. B* **1998**, *57*, 12964; (c) Pasveer, W. F.; Cottaar, J.; Tanase, C.; Coehoorn, R.; Bobbert, P. A.; Blom, P. W. M.; de Leeuw, D. M.; Michels, M. A. J. *Phys. Rev. Lett.* **2005**, *94*, 206601.
(36) Zhang, X.; Richter, L. J.; DeLongchamp, D. M.; Kline, R. J.; Hammond, M. R.; McCulloch, I.; Heeney, M.; Ashraf, R. S.; Smith, J. N.; Anthopoulos, T. D.; Schroeder, B.; Geerts, Y. H.; Fischer, D. A.; Toney, M. F. *J. Am. Chem. Soc.* **2011**, *133*, 15073.
(37) Rivnay, J.; Toney, M. F.; Zheng, Y.; Kauvar, I. V.; Chen, Z.; Wagner, V.; Facchetti, A.; Salleo, A. *Adv. Mater.* **2010**, *22*, 4359.
(38) Huang, W.; Yang, B.; Sun, J.; Liu, B.; Yang, J.; Zou, Y.; Xiong, J.; Zhou, C.; Gao, Y. *Org. Electron.* **2014**, *15*, 1050.
(39) Dong, H.; Bo, Z.; Hu, W. *Macromol. Rapid Commun.* **2011**, *32*, 649.
(40) (a) Gong, X.; Tong, M.; Xia, Y.; Cai, W.; Moon, J. S.; Cao, Y.; Yu, G.; Shieh, C.-L.; Nilsson, B.; Heeger, A. J. *Science* **2009**, *325*, 1665; (b) Liu, C.-H.; Chang, Y.-C.; Norris, T. B.; Zhong, Z. *Nat. Nano.* **2014**, *9*, 273.

Table of Contents artwork